TRANSACTIONS OF THE
AMERICAN MATHEMATICAL SOCIETY
Volume 369, Number 3, March 2017, Pages 2029–2048
http://dx.doi.org/10.1090/tran/6807
Article electronically published on May 17, 2016

GLOBAL DYNAMICS OF A YANG-MILLS FIELD ON AN ASYMPTOTICALLY HYPERBOLIC SPACE

PIOTR BIZOŃ AND PATRYK MACH

Abstract. We consider a spherically symmetric (purely magnetic) $SU(2)$ Yang-Mills field propagating on an ultrastatic spacetime with two asymptotically hyperbolic regions connected by a throat of radius α. Static solutions in this model are shown to exhibit an interesting bifurcation pattern in the parameter α. We relate this pattern to the Morse index of the static solution with maximal energy. Using a hyperboloidal approach to the initial value problem, we describe the relaxation to the ground state solution for generic initial data and unstable static solutions for initial data of codimension one, two, and three.

1. Introduction and setup

The evolution of a Yang-Mills field in a four-dimensional Minkowski spacetime is rather uneventful; all solutions starting from smooth initial data at $t = 0$ remain smooth forever [1] and decay to zero as $t \to \infty$ [2, 3]. In a globally hyperbolic four-dimensional curved spacetime the evolution can be more intricate: although singularities cannot develop [4], there may exist nontrivial stationary attractors giving rise to critical phenomena at the boundaries of their basins of attraction, as was shown for the Schwarzschild background [5].

Here we consider the evolution of a spherically symmetric $SU(2)$ Yang-Mills field on an ultrastatic spacetime $(\mathcal{M}, g)$ with the manifold $\mathcal{M} = \{(t, r) \in \mathbb{R}^2, (\vartheta, \varphi) \in S^2\}$ and metric

$$g = -dt^2 + dr^2 + \alpha^2 \cosh^2 r \, d\omega^2 , \tag{1}$$

where $d\omega^2 = d\vartheta^2 + \sin^2\vartheta \, d\varphi^2$ is the round metric on the unit 2-sphere. The hypersurfaces $t = \text{const}$ are three-dimensional asymptotically hyperbolic cylinders that are symmetric under the reflection $r \to -r$. The neck, $r = 0$, of this hyperbolic wormhole is a minimal surface of area $4\pi\alpha^2$. The Ricci scalar of (1) is equal to $R(g) = -6 + (2 + 2\alpha^{-2}) \operatorname{sech}^2 r$.

We are interested in an $SU(2)$ Yang-Mills field propagating on $(\mathcal{M}, g)$. The gauge potential $A_\mu = A^a_\mu \tau_a$ takes values in the Lie algebra $su(2)$, where the generators τ_a satisfy $[\tau_a, \tau_b] = i\epsilon_{abc}\tau_c$. In terms of the Yang-Mills field tensor, $F_{\mu\nu} = \nabla_\mu A_\nu - \nabla_\nu A_\mu + [A_\mu, A_\nu]$, the lagrangian density reads

$$\mathcal{L} = \operatorname{Tr}\left(F_{\alpha\beta} F_{\mu\nu} g^{\alpha\mu} g^{\beta\nu}\right) \sqrt{-\det(g_{\mu\nu})}. \tag{2}$$

Received by the editors March 17, 2015.
2010 *Mathematics Subject Classification.* Primary 35Q75.

For the Yang-Mills potential we assume the spherically symmetric purely magnetic ansatz

$$A = W(t,r)\,\eta + \tau_3 \cos\vartheta d\varphi\,, \quad \text{where} \quad \eta = \tau_1 d\vartheta + \tau_2 \sin\vartheta\, d\varphi\,, \tag{3}$$

which gives the Yang-Mills field tensor

$$F = \partial_t W dt \wedge \eta + \partial_r W dr \wedge \eta - (1-W^2)\,\tau_3\, d\vartheta \wedge \sin\vartheta\, d\varphi\,. \tag{4}$$

Note that the vacuum state $W = \pm 1$ is two-fold degenerate. Inserting ansatz (4) into (2) we get the reduced lagrangian density

$$\mathcal{L} = -\frac{1}{2}\,(\partial_t W)^2 + \frac{1}{2}\,(\partial_r W)^2 + \frac{(1-W^2)^2}{4\alpha^2 \cosh^2 r}\,. \tag{5}$$

Hereafter it is convenient to define the constant ℓ by $\ell(\ell+1) = \alpha^{-2}$. Then, the Euler-Lagrange equation derived from (5) reads

$$\partial_{tt} W = \partial_{rr} W + \frac{\ell(\ell+1)}{\cosh^2 r}\, W(1-W^2)\,, \tag{6}$$

and the associated conserved energy is

$$E = \frac{1}{2}\int_{-\infty}^{\infty} \left((\partial_t W)^2 + (\partial_r W)^2 + \frac{\ell(\ell+1)}{2\cosh^2 r}\,(1-W^2)^2 \right) dr\,. \tag{7}$$

The Yang-Mills equation (6) is a bona fide $1+1$ dimensional semilinear wave equation for which it is routine to show that solutions starting at $t = 0$ from smooth finite-energy initial data remain smooth for all future times.[1]

The goal of this paper is to describe the asymptotic behavior of solutions for $t \to \infty$. Due to the dissipation of energy by dispersion, solutions are expected to settle down to critical points of the potential energy, i.e., static solutions. Before studying the evolution, in the following two sections we describe the static sector of the model.

2. Static solutions

Time-independent solutions $W = W(r)$ of equation (6) satisfy the ordinary differential equation

$$W'' + \frac{\ell(\ell+1)}{\cosh^2 r}\, W(1-W^2) = 0\,. \tag{8}$$

Due to the reflection symmetry $W \to -W$, all solutions (except the reflection invariant solution $W_* = 0$) come in pairs. In the following, each pair $\pm W$ will be counted as one solution. Besides W_*, the second constant solution is $W_0 = 1$, which is the ground state with zero energy. These two constant solutions will play the key role in our analysis.[2]

[1] As we have mentioned above, global regularity holds for the Yang-Mills equation on any four-dimensional globally hyperbolic spacetime [4]. However the proof of this fact is highly nontrivial already in Minkowski spacetime [1].

[2] Note that, in contrast to the Yang-Mills model in a flat space, W_* is a smooth, finite energy solution; it is a hyperbolic analogue of Wheeler's "charge without charge" configuration [6] with two magnetic charges of opposite signs ± 1 sitting at $r = \pm\infty$.

We will show below that as ℓ increases from zero, nonconstant static solutions with finite energy bifurcate from W_* at each positive integer value of ℓ. These solutions are either odd or even so it is sufficient to analyze them for $r \geq 0$. The odd solutions are parametrized by $W'(0)$ and the even solutions are parametrized by $W(0)$. Near $r = \infty$ these solutions belong to the one-parameter family of solutions

$$W(r) = W_\infty + \mathcal{O}(e^{-2r}), \tag{9}$$

which are analytic in the parameter W_∞ and e^{-2r}. Smooth solutions of (8) satisfying (9) will be referred to as regular solutions.

Theorem 1. *Let n be a nonnegative integer. For $2n < \ell < 2n+2$ there are exactly n regular even solutions $W_{2n}(r)$ and for $2n+1 < \ell < 2n+3$ there are exactly n regular odd solutions $W_{2n+1}(r)$ (the subscript of W counts the number of zeros of $W(r)$ on the real line).*

Proof. We consider only the odd solutions (the proof of existence of even solutions is analogous). The odd solution with $b = W'(0)$ will be denoted by $W(r, b)$. Without loss of generality we assume that $b \geq 0$. The proof, following the lines of the shooting argument given in [7], proceeds in three steps:

Step 1 (a priori global behavior). It follows from (8) that $W(r)$ cannot have a maximum (resp. minimum) for $W > 1$ (resp. $W < -1$), so once $W(r, b)$ leaves the strip $|W| < 1$, it cannot reenter it. Suppose that $|W(r, b)| < 1$ for all r. We define the functional

$$Q(r) = \cosh^2 r\, W'^2 - \frac{\ell(\ell+1)}{2}(1 - W^2)^2 . \tag{10}$$

From (8) we have

$$Q'(r) = \sinh(2r)\, W'^2 , \tag{11}$$

hence $Q(r)$ is increasing for $r \geq 0$. It is easy to see that if $Q(r_0) > 0$ for some r_0, then $|W(r_1, b)| = 1$ for some $r_1 > r_0$. Thus, $Q(r) < 0$ for all $r \geq 0$, in particular $Q(0) = 2b^2 - \ell(\ell+1) < 0$. Together with (11) this implies that $\lim_{r\to\infty} Q(r) \leq 0$ exists, and therefore $\lim_{r\to\infty} Q'(r) = 0$, which is equivalent to $\lim_{r\to\infty} e^r W'(r) = 0$. The existence of $\lim_{r\to\infty} Q(r)$ and (10) imply in turn that $W_\infty := \lim_{r\to\infty} W(r)$ exists. Concluding, the solution for which $|W(r, b)| < 1$ for all r has the desired asymptotic behavior (9).

Step 2 (behavior of solutions for small b). Inserting $W(r) = bw(r)$ into (8) and taking the limit $b \to 0$ we get

$$w'' + \frac{\ell(\ell+1)}{\cosh^2 r}\, w = 0, \quad w(0) = 0, \quad w'(0) = 1 . \tag{12}$$

The solution of this limiting equation is given by the Legendre function

$$w_L(r) = \tanh r\, {}_2F_1\left(\frac{1-\ell}{2}, \frac{\ell+2}{2}, \frac{3}{2}; \tanh^2 r\right), \tag{13}$$

which oscillates $n+1$ times around zero (i.e., has $n+1$ zeros) for $r > 0$, where $2n+1$ is the smallest odd number less than ℓ, and then diverges to $(-1)^{n+1}\infty$ (or goes to $(-1)^{n+1}$ if $2n+3 = \ell$). By continuity, for b small enough, $W(r, b)$ behaves in the same manner on compact intervals.

Step 3 (shooting argument). We define the set

$$B_1 = \{b \,|\, W(r,b) \text{ grows monotonically to } W(r_0,b) = 1 \text{ at some } r_0\}.$$

We know from Step 1 that the set B_1 is nonempty because all solutions $W(r,b)$ with $b > \sqrt{\ell(\ell+1)/2}$ belong to it. On the other hand, we know from Step 2 that if $\ell > 1$, then the set B_1 is bounded from below by a positive constant. Thus, $b_1 = \inf B_1$ is strictly positive. The solution $W(r,b_1)$ cannot touch $W = 1$ for a finite r because the same would be true for nearby orbits, violating the definition of b_1. Therefore, $|W(r,b)| < 1$ for all r and hence, by Step 1, $W(r,b_1)$ is the desired first regular odd solution with one zero. We denote it by W_1.

Next, consider the solution $W(r,b_1-\varepsilon)$ for a small positive ε. From the definition of b_1 it follows that $W(r,b_1-\varepsilon)$ attains a local maximum $W(r_0) < 1$ for some r_0. It is not difficult to show that for sufficiently small ε the solution $W(r,b_1-\varepsilon)$, after reaching the maximum at r_0, decreases monotonically to $W(r_1) = -1$ for some $r_1 > r_0$ (we omit the proof of this fact because it is very similar to the analogous proof given in [7]). This means that the set

$$B_3 = \{b \,|\, W(r,b) \text{ grows monotonically to a maximum at some } r_0 \text{ and then monotonically decreases to } W(r_1,b) = -1 \text{ at some } r_1 > r_0\}$$

is nonempty. We know from Step 2 that if $\ell > 3$, then $b_3 = \inf B_3$ is strictly positive. By the same argument as above, the solution $W(r,b_3)$ stays in the strip $|W| < 1$ for all r and gives the desired regular odd solution with three zeros. We denote it by $W_3(r)$.

The subsequent solutions $W_{2n+1}(r)$ can be obtained by iterating the argument as long as $2n+1 < \ell$. □

The first few solutions W_n computed numerically are shown in Figure 1.

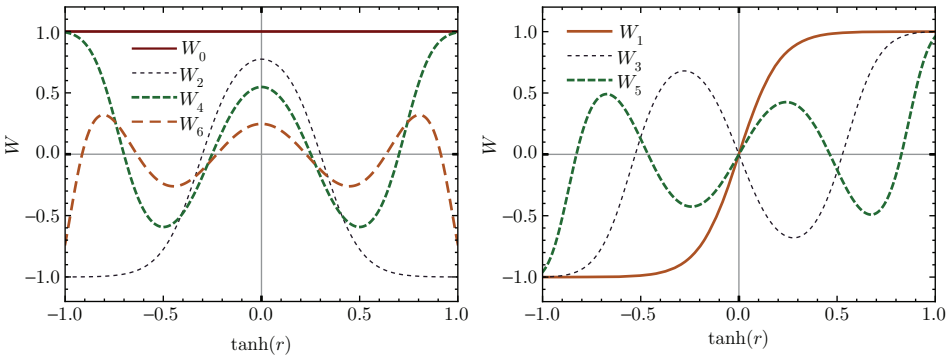

FIGURE 1. Static solutions W_n for $\ell = 6.5$. The r-axis is compactified to the interval $[-1,1]$ by using $\tanh r$.

We conclude this section with a few remarks concerning the properties of static solutions.

Remark 1. Multiplying (8) by W and integrating by parts we get the virial identity

$$\int_{-\infty}^{\infty} W'^2 dr = \ell(\ell+1) \int_{-\infty}^{\infty} W^2(1-W^2)\operatorname{sech}^2 r \, dr. \tag{14}$$

Inserting this into (7) gives for static solutions

$$E = \frac{\ell(\ell+1)}{4} \int_{-\infty}^{\infty} (1 - W^4) \operatorname{sech}^2 r \, dr \,. \tag{15}$$

This shows that the energies $E_n := E(W_n)$ are bounded from above by the energy $E_* := E(W_*) = \ell(\ell+1)/2$ (see Figure 2).

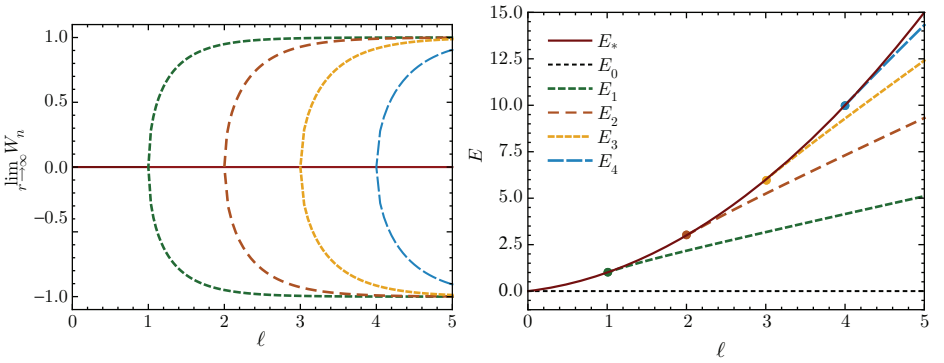

FIGURE 2. Left panel: The bifurcation diagram showing a sequence of supercritical pitchfork bifurcations at integer values of ℓ. Right panel: The energies E_n are shown to bifurcate from the parabola $E_* = \ell(\ell+1)/2$ at integer values of ℓ. The bifurcation points are marked with dots.

Remark 2. Multiplying (8) by W' and integrating by parts we get an identity

$$\int_{-\infty}^{\infty} \tanh r \operatorname{sech}^2 r \, (1 - W^2)^2 \, dr = 0 \,, \tag{16}$$

which is trivially satisfied by odd and even solutions and suggests that nonsymmetric solutions do not exist. However proving that is an open problem.

Remark 3. For large values of ℓ one can obtain an analytic approximation of the solution $W_1(r)$ as follows. Let $y = \sqrt{\ell(\ell+1)}r$ and $\bar{W}(y) = W(r)$. Then, in the limit $\ell \to \infty$ equation (8) reduces to $\bar{W}'' + \bar{W}(1 - \bar{W}^2) = 0$. The separatrix solution of this limiting equation $\bar{W}_1(y) = \tanh(y/\sqrt{2})$ gives the approximation

$$W_1(r) \simeq \tanh\left(\sqrt{\frac{\ell(\ell+1)}{2}} r\right) \quad \text{for} \quad \ell \gg 1 \,. \tag{17}$$

Remark 4. The static energy

$$E = \frac{1}{2} \int_{-\infty}^{\infty} \left(W'^2 + \frac{\ell(\ell+1)}{2 \cosh^2 r} (1 - W^2)^2 \right) dr \tag{18}$$

is an example of an energy functional with the following properties: a) it is invariant under a discrete Z_2 symmetry (here, the reflection $W \to -W$), b) the fixed point of this symmetry (here, W_*) is a critical point with maximal energy, c) it satisfies the Palais-Smale condition. Corlette and Wald conjectured[3] in [8], using Morse

[3]Actually, this conjecture was not stated explicitly in [8], but it follows naturally from the argument given there.

theory arguments, that for such functionals the number of critical points (counted without multiplicity) with energy below $E(W_*)$ is equal to the Morse index of W_* (i.e. the number of negative eigenvalues of the Hessian of E at W_*). We will show below that when $\ell < 1$ the Morse index of W_* is equal to 1 and, as ℓ grows, it increases by one at each integer value of ℓ. Thus, according to the conjecture of Corlette and Wald, for a given ℓ there should be exactly n (besides W_*) critical points of the energy functional, where n is the largest integer less than ℓ. This is in perfect agreement with Theorem 1, provided that there are no nonsymmetric critical points.

3. Linearized perturbations

In this section we determine the linear stability properties of static solutions $W_n(r)$. This step is essential for understanding the role of static solutions in the evolution. Following the standard procedure we seek solutions of equation (6) in the form $W(t,r) = W_n(r) + w(t,r)$. Hereafter, in the case of W_* the subscript n should be replaced by $*$. Neglecting quadratic and cubic terms in w, we obtain the evolution equation for linear perturbations

$$\partial_{tt} w - \partial_{rr} w + V_n(r)\, w = 0\,, \quad V_n(r) = \frac{\ell(\ell+1)}{\cosh^2 r}\,(3W_n^2(r) - 1)\,. \tag{19}$$

Separation of time dependence $w(t,r) = e^{\lambda t} v(r)$ yields the eigenvalue problem for the one-dimensional Schrödinger operator

$$L_n\, v := (-\partial_{rr} + V_n(r))\; v = \sigma\, v, \quad \sigma = -\lambda^2\,. \tag{20}$$

Since the potential $V_n(r)$ is an even function of r, the eigenfunctions are alternately even and odd. We claim that the operator L_n has exactly n negative eigenvalues, independently of ℓ. For $n = 0$ this is obvious because the potential $V_0(r) = 2\ell(\ell+1)\operatorname{sech}^2 r$ is everywhere positive. For $n \geq 1$ we can obtain a lower bound as follows. Consider the function $v_n(r) = \cosh r\, W_n'(r)$. Multiplying (8) by $\cosh^2 r$ and then differentiating, we find that $L_n\, v_n = -v_n$; hence v_n is the eigenfunction to the eigenvalue $\sigma = -1$. Since $W_n(r)$ has $(n-1)$ local extrema, the eigenfunction $v_n(r)$ has $(n-1)$ zeros, which implies by the Sturm oscillation theorem that there are exactly $(n-1)$ eigenvalues below -1. Consequently, the operator L_n has at least n negative eigenvalues. Numerics shows that there are no eigenvalues in the interval $-1 < \sigma < 0$, indicating that the above lower bound is sharp, but we have not been able to prove that (see, however, Remark 5 below).

In the case of $W_* = 0$ the potential $V_* = -\ell(\ell+1)\operatorname{sech}^2 r$ is the exactly solvable Pöschl-Teller potential [9], which is known to have $n+1$ negative eigenvalues $\sigma_j = -(\ell - j)^2$ for $j = 0, 1, \ldots, n$, where n is the largest integer less than ℓ. In particular, for $\ell < 1$ there is only one negative eigenvalue. At each positive integer value of ℓ a new zero energy resonance emerges from the bottom of the continuous spectrum and becomes a negative eigenvalue as ℓ grows.

Remark 5. From the structure of the spectrum of perturbations around W_* it follows, using bifurcation theory, that at each positive integer value of ℓ there is a supercritical pitchfork bifurcation at which a pair of solutions $\pm W_n$ with $n = \ell$ is born. This gives an alternative "soft" argument for existence of solutions W_n in some small intervals $n < \ell < n + \varepsilon$. In these intervals the solutions W_n

are guaranteed to have one unstable mode less than W_*, in agreement with our conjecture above.

In order to understand the evolution in the neighbourhood of static solutions, besides unstable modes, one needs to determine the quasinormal modes. They are defined as solutions of the eigenvalue equation (20) with $\mathrm{Re}(\lambda) < 0$ and the outgoing wave conditions $v(r) \sim \exp(\mp\lambda r)$ for $r \to \pm\infty$. As the concept of quasinormal modes is inherently related to the loss of energy by radiation, the unitary evolution (19) and the associated self-adjoint eigenvalue problem (20) do not provide a natural setting for analysing quasinormal modes, both from the conceptual and computational viewpoints. For this reason we postpone the discussion of quasinormal modes until the next section where a new nonunitary formulation will be introduced.

4. Hyperboloidal formulation

We define new coordinates

$$\tau = t - \log(\cosh r)\,, \quad x = \tanh r\,. \tag{21}$$

Then metric (1) takes the form

$$g = (1-x^2)^{-1}\,\hat{g}, \quad \hat{g} = -(1-x^2)d\tau^2 - 2x\,d\tau dx + dx^2 + \alpha^2\,d\omega^2\,. \tag{22}$$

The conformal metric $\hat{g}$ is diffeomorphic to the Nariai metric [10], which is a product of the two-dimensional de Sitter metric and the round metric on the 2-sphere. It has constant positive scalar curvature $R(\hat{g}) = 2 + 2/\alpha^2$. The manifold $\mathcal{M}$ is the static patch of $\mathrm{dS}_2 \times S^2$ whose cosmological horizons (null hypersurfaces $x = \pm 1$) correspond to null infinities of $\mathcal{M}$. In $(\mathcal{M}, \hat{g})$ the spacelike hypersurfaces $\tau =$ const are three-dimensional cylinders $R \times S^2$. Note that the Yang-Mills equation is conformally invariant in four dimensions, hence it takes the same form on $(\mathcal{M}, g)$ and $(\mathcal{M}, \hat{g})$. The hypersurfaces $\tau =$ const are "hyperboloidal", that is, they are spacelike hypersurfaces that approach the "right" future null infinity $\mathcal{J}_R^+$ along outgoing null cones of constant retarded time $t-r$ and the "left" future null infinity $\mathcal{J}_L^+$ along outgoing null cones of constant advanced time $t+r$.

We recall that the hyperboloidal approach to the initial value problem was introduced by Friedrich in his studies of asymptotically flat solutions of Einstein's equations [11]. More recently, this approach has been developed and applied by Zenginoğlu [12,13], who emphasized its advantages over the traditional approaches (see also [14]). Until now, as far as we know, the hyperboloidal approach has not been used in the context of asymptotically hyperbolic spacetimes.

In terms of the coordinates (τ, x) equation (6) becomes[4]

$$\partial_{\tau\tau}W + 2x\partial_{\tau x}W + \partial_\tau W = \partial_x\left((1-x^2)\partial_x W\right) + \ell(\ell+1)W(1-W^2)\,. \tag{23}$$

The principal part of this hyperbolic equation degenerates at the endpoints $x = \pm 1$ to $\partial_\tau(\partial_\tau \pm 2\partial_x)W$, hence there are no ingoing characteristics at the boundaries and consequently no boundary conditions are required or, for that matter, allowed. This, of course, reflects the fact that no information comes in from the future null infinities.

[4]Hereafter we abuse notation and use the same letter W for the dependent variable in coordinates (t, r) and (τ, x).

Multiplying (23) by $\partial_\tau W$ we obtain the local conservation law

$$\partial_\tau \rho + \partial_x f = 0\,, \tag{24}$$

where

$$\rho = \frac{1}{2}\left((\partial_\tau W)^2 + (1-x^2)(\partial_x W)^2 + \frac{\ell(\ell+1)}{2}\,(1-W^2)^2\right)\,, \tag{25}$$

$$f = x\,(\partial_\tau W)^2 - (1-x^2)\partial_\tau W \partial_x W\,. \tag{26}$$

Integrating the conservation law (24) over a $\tau =$ const hypersurface we get the energy balance

$$\frac{d\mathcal{E}}{d\tau} = -(\partial_\tau W(\tau,-1))^2 - (\partial_\tau W(\tau,1))^2\,, \tag{27}$$

where

$$\mathcal{E}(\tau) = \int_{-1}^{1} \rho\, dx \tag{28}$$

is the Bondi-type energy.[5] Formula (27) expresses the radiative loss of energy through future null infinities. Since the energy $\mathcal{E}(\tau)$ is positive and monotone decreasing, it has a nonnegative limit for $\tau \to \infty$. It is natural to expect that this limit is given by the energy of a static endstate of evolution.[6] We thus see that the hyperboloidal approach is ideally suited for studying the relaxation processes which are governed by the dispersive dissipation of energy.

In the remainder of the paper we describe in detail the asymptotic behavior of solutions to (23) for smooth, finite energy initial data. To this end, we first return to the analysis of linearized perturbations and redo it in the hyperboloidal framework. Substituting $W(\tau,x) = W_n(x) + w(\tau,x)$ into (23) and linearizing, we obtain the equation

$$\partial_{\tau\tau} w + 2x\partial_{\tau x} w + \partial_\tau w = \partial_x\left((1-x^2)\partial_x w\right) + \ell(\ell+1)(1-3W_n^2)\,w\,, \tag{29}$$

which for $w(\tau,x) = e^{\lambda\tau}u(x)$ yields the eigenvalue problem for the quadratic pencil of linear operators

$$(A_n + \lambda\, B + \lambda^2 I)\,u = 0\,, \tag{30}$$

where

$$A_n = -\partial_x\left((1-x^2)\partial_x\right) + \ell(\ell+1)(3W_n^2(x)-1), \quad B = 2x\partial_x + 1\,.$$

[5]Note that $\partial_\tau = \partial_t$. Hence for time-independent fields the Bondi-type energy $\mathcal{E}$ is equal to the standard energy E defined in (7).

[6]In order to turn this expectation into a proof, it would suffice to show that the 'kinetic energy' $\frac{1}{2}\int_{-1}^{1}(\partial_\tau W)^2\,dx$ must tend to zero as $\tau \to \infty$.

Here A_n is the self-adjoint operator (corresponding to the operator L_n defined in (20)), while the operator B is skew-symmetric. Thus, if λ is an eigenvalue,[7] so is its complex conjugate $\bar{\lambda}$. In this setting the quantization condition for the eigenvalues amounts to the requirement that the eigenfunctions be smooth at the endpoints $x = \pm 1$. Note that here, in contrast to the self-adjoint formulation from section 3, both unstable and stable (quasinormal) modes are treated on equal footing as genuine eigenfunctions.[8]

For constant solutions, $W_* = 0$ and $W_0 = 1$, one can solve the quadratic eigenvalue problem (30) using the power series method. In the case of W_*, inserting the power series

$$u(x) = \sum_{j=0}^{\infty} c_j x^j \tag{31}$$

into (30) we obtain the recurrence relation

$$c_{j+2} = \frac{(j+\lambda+\ell+1)(j+\lambda-\ell)}{(j+2)(j+1)}\, c_j\,, \tag{32}$$

where $c_0 = 1$, $c_1 = 0$ for even solutions and $c_0 = 0$, $c_1 = 1$ for odd solutions. Using the ratio test and the Gauss convergence criterion it is easy to see that the function defined by the power series (31) is smooth for $|x| < 1$, but it is not smooth at $x = \pm 1$ unless the series is truncated for a finite j. The truncation condition gives two sequences of eigenvalues:

$$\lambda^{\pm}_{*,j} = -j - \frac{1}{2} \pm (\ell + \frac{1}{2}), \qquad j = 0, 1, \ldots. \tag{33}$$

The corresponding eigenfunctions $u^{\pm}_{n,j}$ are even and odd polynomials of order j for even and odd j, respectively. It follows from (33) that W_* has one (even) unstable mode ($\lambda^{+}_{*,0} = \ell, u^{+}_{*,0} = 1$), if $\ell < 1$, and as ℓ increases, it picks up new unstable modes at each integer value of ℓ. Thus, for a given ℓ there are exactly $n+1$ unstable modes where n is the largest integer less than ℓ.

In the case of W_0 the recurrence relation is

$$c_{j+2} = \frac{\lambda^2 + (2+j)\lambda + j^2 + j + 2\ell(\ell+1)}{(j+2)(j+1)}\, c_j\,, \tag{34}$$

and the truncation condition yields two sequences of eigenvalues:

$$\lambda^{\pm}_{0,j} = -j - \frac{1}{2} \pm \frac{1}{2}\sqrt{1 - 8\ell(\ell+1)}, \qquad j = 0, 1, \ldots. \tag{35}$$

All the eigenvalues have a negative real part (in agreement with the analysis in section 3). An imaginary part is nonzero if $\ell > (\sqrt{6} - 2)/4$.

[7] Mind the change of terminology: in the previous section $\sigma = -\lambda^2$ was referred to as the eigenvalue, while for the quadratic pencil λ is called an eigenvalue.

[8] To our knowledge, the advantages of the hyperboloidal foliations in the definition and analysis of quasinormal modes were first pointed out by Schmidt [15]. More recently, this idea was implemented numerically in [5] and, in the case of asymptotically anti-de Sitter black holes, was independently developed rigorously by Warnick in the framework of semigroup theory [16].

The power series method is not applicable to the solutions W_n with $n \geq 1$ because they are not known in closed form. Hence in order to compute their spectrum of perturbations one has to resort to numerical methods, for example the shooting method[9] (see [17]). In this case we shall adopt the following convention for the ordering of eigenvalues:

$$\lambda_{n,0} > \cdots > \lambda_{n,n-1} = 1 > 0 > \mathrm{Re}(\lambda_{n,n}) > \mathrm{Re}(\lambda_{n,n+1}) > \ldots .$$

Summarizing, the following picture emerges from our analysis. For a given ℓ there are $n+2$ static solutions $W_0, W_1, \ldots, W_n, W_*$, where n is the largest integer less that ℓ. Due to the global-in-time regularity of solutions and monotone decrease of the energy $\mathcal{E}$, the static solutions are expected to be the only possible endstates of evolution for any smooth, finite energy initial data. Since the solution W_n has n unstable modes (or $n+1$ in the case of W_*), only W_0 is a generic attractor, while the solutions W_n with $n \geq 1$ are unstable attractors of codimension n (or $n+1$ in the case of W_*). The analytic and numerical evidence supporting this picture will be given in the following section where we describe in detail the dynamics of convergence to the static attractors.

5. Relaxation to an equilibrium

In this section we solve equation (23) numerically for a variety of smooth, finite energy initial data and different values of ℓ. We use the spectral Galerkin method which appears to be ideally suited to the problem at hand. The implementation of this method is presented in detail in Appendix A. Our goal is to describe quantitatively the process of relaxation to static solutions. We will discuss in turn the relaxation to the generic attractor W_0, the codimension-one attractors W_* (for $\ell \leq 1$) or W_1 (for $\ell > 1$), the codimension-two attractors W_* (for $1 < \ell < 2$) or W_2 (for $\ell > 2$), and the codimension-three attractors W_* (for $2 < \ell < 3$) or W_3 (for $\ell > 3$).

5.1. **Relaxation to W_0.** Generic initial data are expected to evolve towards the static solution W_0; our numerical results confirm this expectation. Figure 3 shows the evolution for $\ell = 7/2$ of sample initial data

$$W(0,x) = T_1(x) + T_4(x) + T_5(x), \quad \partial_\tau W(0,x) = 0\,. \tag{36}$$

Here and in the following, $T_n(x)$ denotes the n-th Chebyshev polynomial. We choose initial data as a simple combination of Chebyshev polynomials because they can be easily implemented in the framework of our numerical method. Note that the first two eigenfunctions around W_0 and W_* are given by the first two Chebyshev polynomials:

$$u^{\pm}_{0,0} = u^{\pm}_{*,0} = T_0 \equiv 1 \quad \text{and} \quad u^{\pm}_{0,1} = u^{\pm}_{*,1} = T_1 \equiv x.$$

This fact will be very convenient in the following, however it should be remembered that it is specific to our choice of the hyperboloidal coordinates (21).

[9] In the case of W_1, the single unstable mode is even, so the least damped stable mode can be easily obtained by solving the linearized equation (29) for some odd initial data and fitting an exponentially damped sinusoid to $w(\tau, x_0)$ at some x_0.

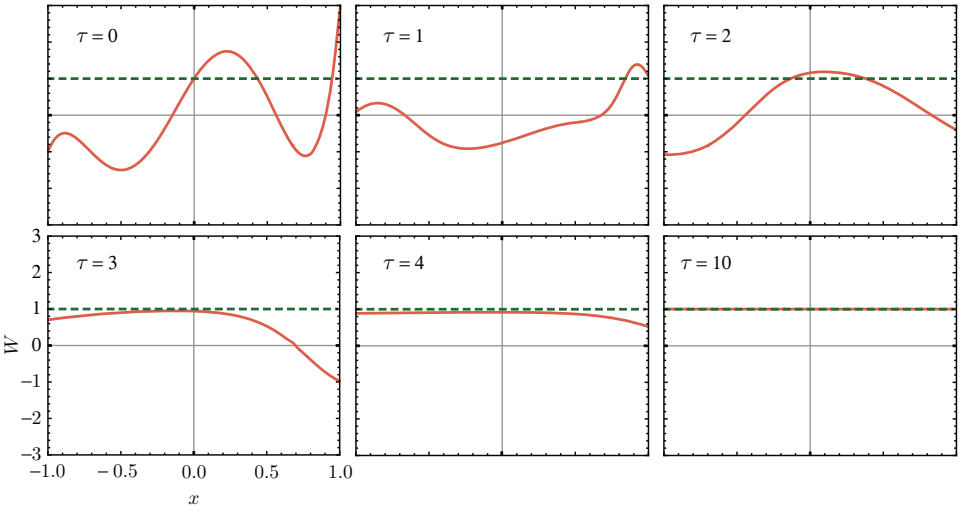

FIGURE 3. Relaxation to W_0 for $\ell = 7/2$ and the initial data (36).

We find that the convergence to W_0 is determined by the least damped mode with the eigenvalue and eigenfunction

$$\lambda^+_{0,0} = -\frac{1}{2} + \frac{1}{2}\sqrt{1 - 8\ell(\ell+1)}\,, \quad u^+_{0,0}(x) = 1\,, \tag{37}$$

that is, for $\tau \to \infty$[10]

$$W(\tau, x) - W_0 \sim \mathrm{Re}\left(A_0 e^{\lambda^+_{0,0}\tau}\right) + \text{subleading terms}\,, \tag{38}$$

where A is a constant depending on the initial data. This asymptotics can be formally derived using the Galerkin approximation of the infinite-dimensional dynamical system (56). To see this, note that the solution $W_0 \equiv 1$ corresponds to the fixed point $a_k = \delta^0_k$ of the system (56). Truncating this system at $N = 2$ we obtain

$$\ddot{a}_0 + \dot{a}_0 - \ell(\ell+1)a_0 + \ell(\ell+1)\left(a_0^3 + \frac{3}{2}a_0 a_1^2\right) = 0, \tag{39a}$$

$$\ddot{a}_1 + 3\dot{a}_1 + (2 - \ell(\ell+1))\,a_1 + \ell(\ell+1)\left(3a_0^2 a_1 + \frac{3}{4}a_1^3\right) = 0. \tag{39b}$$

For this system it is routine to show that the convergence to the fixed point ($a_0 = 1, \dot{a}_0 = 0, a_1 = 0, \dot{a}_1 = 0$) for $\tau \to \infty$ has the form

$$a_0(\tau) \sim 1 + \mathrm{Re}\left(A_0 e^{(-\frac{1}{2} + \frac{1}{2}\sqrt{1-8\ell(\ell+1)})\tau}\right), \tag{40a}$$

$$a_1(\tau) \sim \mathrm{Re}\left(A_1 e^{(-\frac{3}{2} + \frac{1}{2}\sqrt{1-8\ell(\ell+1)})\tau}\right). \tag{40b}$$

Increasing the order N of the Galerkin approximation does not affect the leading order asymptotics of $a_0(\tau)$ and $a_1(\tau)$, and the increasingly faster fall-off of higher coefficients can be calculated systematically term by term; therefore (38) follows. The numerical verification of the asymptotic behavior (40) is shown in Figure 4.

[10]The notation $f(\tau) \sim g(\tau)$ for $\tau \to \infty$ means that $f(\tau)$ is "asymptotically equivalent" to $g(\tau)$, i.e., $\lim_{\tau\to\infty} f(\tau)/g(\tau) = 1$.

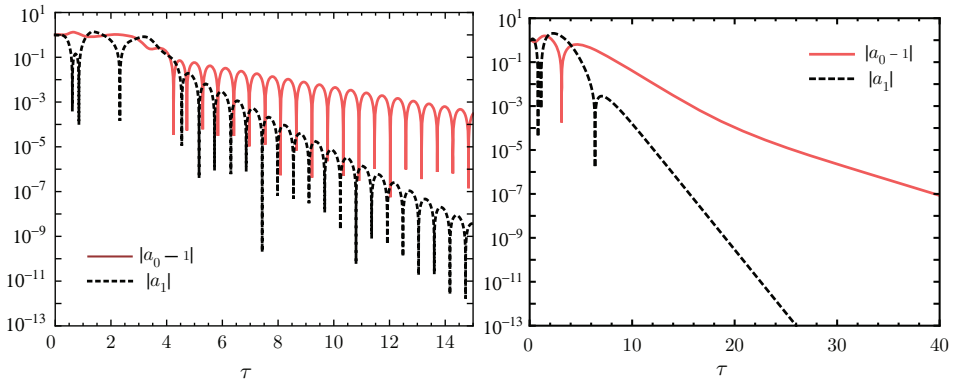

FIGURE 4. Illustration of the asymptotic behavior (40). The plots depict the quantities $|a_0(\tau) - 1|$ and $|a_1(\tau)|$ for the solution with initial data (36). In the oscillatory case $\ell = 7/2$ (left panel) both quantities oscillate with the frequency $5\sqrt{5}/2$ and fall off as $e^{-\tau/2}$ and $e^{-3\tau/2}$, respectively. In the nonoscillatory case $\ell = 1/10$ (right panel) the quantities fall off as $e^{(-5+\sqrt{3})\tau/10}$ and $e^{(-15+\sqrt{3})\tau/10}$, respectively. Note that the asymptotic falloff of $|a_0(\tau)-1|$ becomes visible only for $\tau \gtrsim 25$.

5.2. **Codimension-one attractors.** For odd initial data W_0 cannot be an attractor (because it is even) and the role of an attractor is taken by W_* (if $\ell \leq 1$) or W_1 (if $\ell > 1$). Each of these solutions has one unstable mode, but this mode is even so it does not participate in the evolution of odd initial data. More precisely, odd initial data lie on the stable manifold of W_* if $\ell < 1$, the center-stable manifold of W_* if $\ell = 1$, and the stable manifold of W_1 if $\ell > 1$. Below we describe in turn the relaxation to these attractors.

5.2.1. *Relaxation to W_* for $\ell \leq 1$.* As follows from (33) and (32), the least damped mode has the eigenvalue and eigenfunction

$$\lambda^+_{*,1} = \ell - 1\,, \quad u^+_{*,0}(x) = x\,. \tag{41}$$

For $\ell < 1$, in analogy to (38), we have for $\tau \to \infty$,

$$W(\tau, x) \sim A e^{\lambda^+_{*,1}\tau}\, x + \text{subleading terms}\,. \tag{42}$$

As above, this asymptotic behavior can be formally derived from the Galerkin approximation whose truncation to the first two odd modes reduces to

$$\ddot{a}_1 + 3\dot{a}_1 + (2 - \ell(\ell+1))\, a_1 + 12\dot{a}_3 + 6a_3 + \frac{3}{4}\ell(\ell+1)\left(a_1^3 + a_1^2 a_3 + 2a_3^2 a_1\right) = 0, \tag{43a}$$

$$\ddot{a}_3 + 7\dot{a}_3 + (12 - \ell(\ell+1))\, a_3 + \frac{1}{4}\ell(\ell+1)\left(a_1^3 + 6a_1^2 a_3 + 3a_3^3\right) = 0. \tag{43b}$$

Solving this system asymptotically for $\tau \to \infty$ near the fixed point ($a_1 = \dot{a}_1 = a_3 = \dot{a}_3 = 0$) we get

$$a_1(\tau) \sim A e^{(\ell-1)\tau}, \tag{44a}$$

$$a_3(\tau) \sim -\frac{1}{8}\frac{1+\ell}{1+4\ell} A^3 e^{3(\ell-1)\tau}. \tag{44b}$$

Note that the leading fall-off of $a_3(\tau)$ is governed by the nonlinear term proportional to a_1^3 in equation (43b).

For $\ell = 1$ the eigenvalue $\lambda^+_{*,1} = \ell - 1$ is equal to zero.[11] In this case the coefficient of the term a_1 in equation (43a) vanishes and the decay changes from exponential to power-law, namely

$$a_1(\tau) \sim \pm\frac{\sqrt{5}}{2}\tau^{-1/2}, \tag{45a}$$

$$a_3(\tau) \sim \mp\frac{\sqrt{5}}{32}\tau^{-3/2}. \tag{45b}$$

This nongeneric case is somewhat surprising as it contradicts a naive expectation that the decay is always exponential.[12]

Figure 5 depicts the relaxation to W_* for sample odd initial data

$$W(0,x) = 2T_1(x) + T_5(x), \quad \partial_\tau W(0,x) = 0. \tag{46}$$

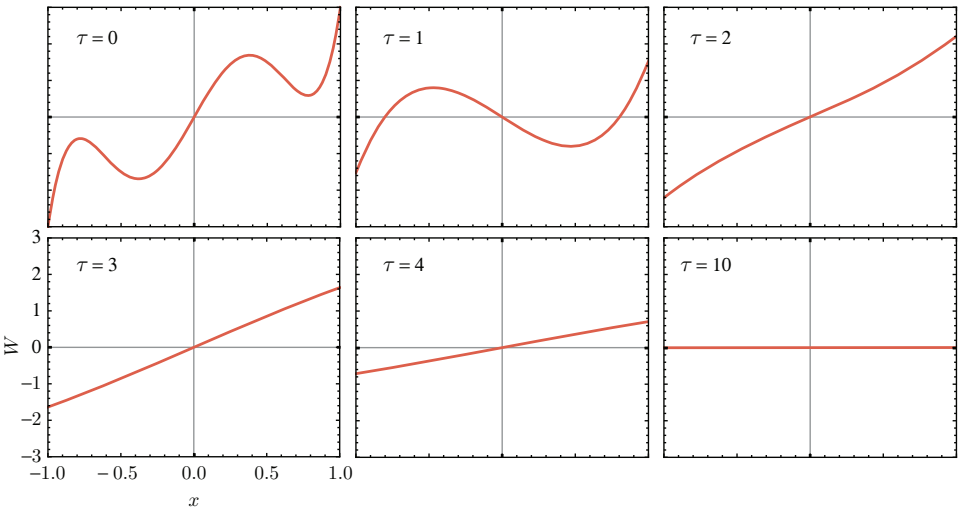

FIGURE 5. Relaxation to W_* for $\ell = 1/8$ and odd initial data (46).

[11] In the framework of the self-adjoint problem (20) this corresponds to the presence of the zero energy resonance at the bottom of the continuous spectrum.

[12] A similar power-law decay occurs for other integer values of ℓ for specially prepared odd initial data.

Increasing the order of the Galerkin approximation does not affect the asymptotics (44) and (45). The numerical verification of these formulae is shown in Figure 6.

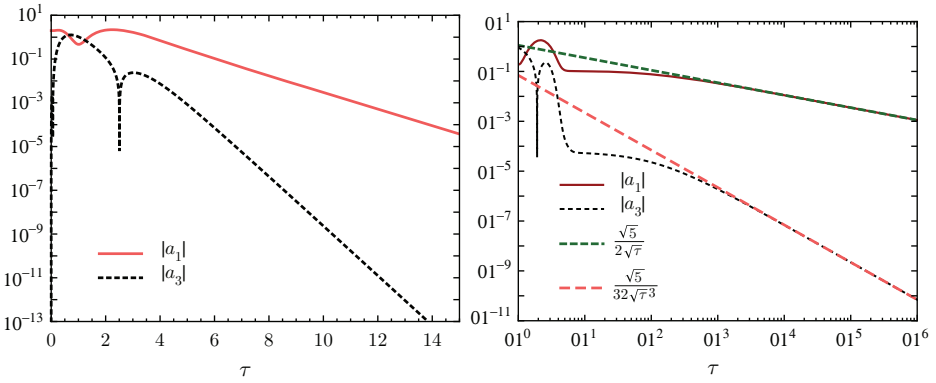

FIGURE 6. Illustration of the asymptotics (44) and (45). The plots depict the coefficients $|a_1(\tau)|$ and $|a_3(\tau)|$ for the solution with initial data (46). The left panel shows the case $\ell = 1/8$. As expected, the coefficients $|a_1(\tau)|$ and $|a_3(\tau)|$ decay as $Ae^{-7\tau/8}$ and $(3A^3/32)e^{-21\tau/8}$, with $A \approx 18.8$. The right panel, using the double logarithmic scale, shows the nongeneric case $\ell = 1$. To make the predicted asymptotic power-law behavior of $|a_1(\tau)|$ and $|a_3(\tau)|$ more visible, we superimpose the graphs of $\sqrt{5}/(2\sqrt{\tau})$ and $\sqrt{5}/(32\sqrt{\tau}^3)$.

5.2.2. *Relaxation to W_1 for $\ell > 1$.* The single unstable mode around W_1 is even, hence it is not present in the evolution of odd initial data. Therefore, in this case we have

$$W(\tau, x) - W_1(x) \sim Ae^{-\gamma_1 \tau} \sin(\omega_1 \tau + \delta)\, u_{1,1}(x) + \dots , \tag{47}$$

where $\gamma_1 = -\mathrm{Re}(\lambda_{1,1})$, $\omega_1 = \mathrm{Im}(\lambda_{1,1})$ and A, δ are constants. Figures 7 and 8 show the numerical results confirming the asymptotic behavior (47) for $\ell = 7/2$ and the initial data (46).

5.3. **Higher codimension attractors.** Thanks to the reflection symmetry $x \to -x$ of equation (23) it is relatively easy to tune initial data to the stable manifolds of static solutions with two and three unstable modes. For example, consider a one-parameter family of even initial data

$$W(0, x) = -1 + c\, T_2(x), \quad \partial_\tau W(0, x) = 0\,. \tag{48}$$

These data interpolate between the basins of attraction of solutions $-W_0$ (for small values of c, say $c = 0$) and W_0 (for large values of c, say $c = 1$). Using bisection one can determine numerically a critical value $c_* \in [0, 1]$ for which the initial data (48) lie on a borderline between these basins of attraction. It is natural to expect that such data will evolve to the least unstable even solution, i.e. W_* if $\ell < 2$ or W_2 if $\ell > 2$. Numerically c_* cannot be determined exactly, and the corresponding near-critical solution approaches W_* or W_2 (depending on the value of ℓ), stays in its

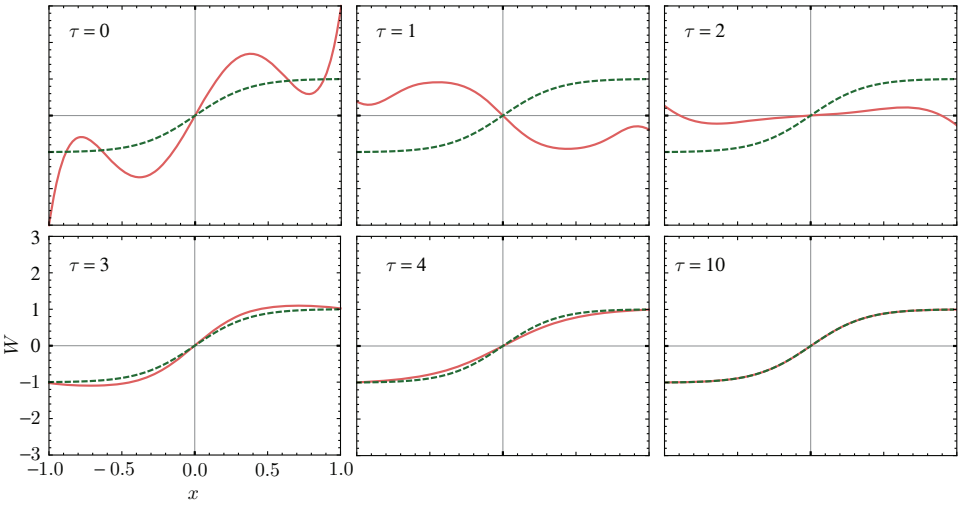

FIGURE 7. Relaxation to W_1 (depicted with the dashed line) for $\ell = 7/2$ and the initial data (46).

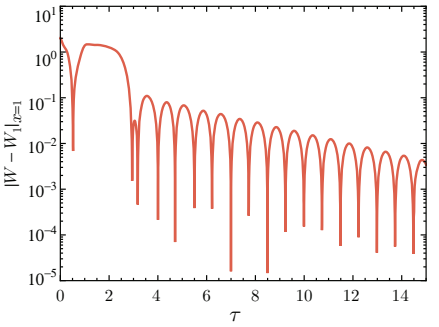

FIGURE 8. Time evolution of $|W - W_1|$ at $x = 1$ for the solution depicted in Figure 7. The parameters of the quasinormal ringdown, $\omega_1 \approx 4.197$ and $\gamma_1 \approx 0.277$, agree with the values determined independently using linear perturbation theory.

neighbourhood for some time and eventually is ejected along the one-dimensional unstable manifold (see Figures 9 and 10). The dynamics of this process can be approximated as follows:

$$W(\tau, x) \sim A_0(c)e^{\ell\tau} + A_2 e^{-(2-\ell)\tau}\,(1 - (2\ell - 1)x) \tag{49}$$

if $\ell < 2$, and

$$W(\tau, x) \sim W_2(x) + A_0(c)e^{\lambda_{2,0}\tau}\,u_{2,0}(x) + A_2 e^{-\gamma_2\tau}\,\sin(\omega_2\tau + \delta)\,u_{2,2}(x) \tag{50}$$

if $\ell > 2$, where $\gamma_2 = -\mathrm{Re}(\lambda_{2,2})$ and $\omega_2 = \mathrm{Im}(\lambda_{2,2})$. For critical initial data $A_0(c_*) = 0$, however, in practice there is always a small admixture of the unstable mode, and therefore W_* and W_2 are only intermediate attractors whose lifetimes scale with c as $-\frac{1}{\gamma}\ln|c - c_*|$, where $\gamma = \ell$ in the case of W_* and $\gamma = \lambda_{2,0}$ in the case of W_2.

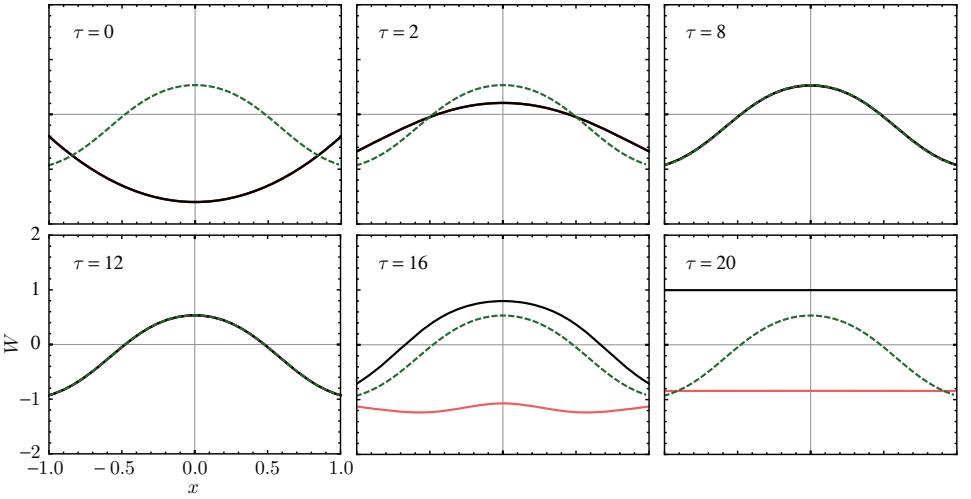

FIGURE 9. Snapshots from the evolution of a pair of near critical initial data (48) for $c = c_- = 0.599712304435598$ and $c = c_+ = 0.599712304435599$. By continuous dependence on initial data, these two solutions evolve for some time close together approaching the unstable attractor W_2 (depicted with the dotted line) and eventually tend to -1 and $+1$, respectively.

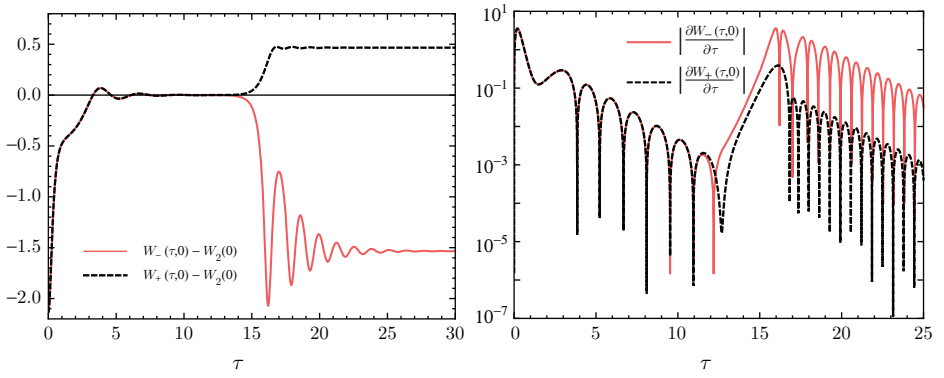

FIGURE 10. The solutions corresponding to near critical parameters $c_\pm$, depicted in Figure 9, are denoted by $W_\pm$. The left and right panels show the time evolution of $W_\pm - W_2$ and $|\partial_\tau W_\pm|$ at $x = 0$, respectively. One can clearly distinguish three phases of evolution: the approach to the unstable attractor W_2 governed by its fundamental quasinormal mode, the departure from W_2 governed by its unstable mode, and finally relaxation to ± 1 governed by its fundamental quasinormal mode.

In a similar manner, one can prepare odd initial data lying on the stable manifold of W_* for $2 < \ell < 3$ or W_3 for $\ell > 3$.

6. Final remarks

The study presented above is part of a bigger project which could be called "Designer PDEs." In this project we play with domains of nonlinear PDEs (mainly wave equations) in order to design toy models for studying various physical phenomena (such as relaxation to equilibrium, weak turbulence, blowup, etc.) in the *simplest* possible settings. The studies of such toy models not only help to understand the underlying phenomena but, in addition, reveal interesting interactions between the geometry of a domain and a nonlinearity. For example, the comparison of dynamics of the Yang-Mills field on the asymptotically hyperbolic wormhole (described in this paper) and the asymptotically flat wormhole (described in the parallel paper [20]) is very instructive in showing how the late time behavior of waves is affected by the asymptotic behavior and the conformal structure of spacetime.

Although equation (6) is very special, we believe that it is representative of a larger class of models in the sense that many of its features, discussed above, are structurally stable with respect to perturbations of the geometry of a domain. We hope that our toy model will serve as a playground for developing new mathematical methods (in particular, tools based on hyperboloidal foliations) for semilinear wave equations on asymptotically hyperbolic spacetimes.

Appendix: Fourier-Galerkin method

To solve equation (23) we use a version of the spectral Fourier-Galerkin method. The solution is expanded in the basis of Chebyshev polynomials of the first kind $\{T_n\}_{n=0,1,\dots}$ as

$$W(\tau,x)=\sum_{n=0}^{\infty}a_n(\tau)T_n(x). \tag{51}$$

The choice of Chebyshev polynomials is suggested by the form of the Chebyshev equation

$$(1-x^2)T_n''(x)-xT_n'(x)+n^2T_n(x)=0.$$

The other obvious choice would be to work with Legendre polynomials. They seem to be even better adjusted to our needs, since the linear part of the right hand side of (23) has the form of the Legendre equation. The reason why we do not work with Legendre polynomials is that the formulae expressing the products of Legendre polynomials as their linear combinations are relatively complicated (cf. [18, 19]). The advantage of using Chebyshev polynomials is that the product of two Chebyshev polynomials can be expressed as

$$T_m(x)T_n(x)=\frac{1}{2}\left(T_{m+n}(x)+T_{|m-n|}(x)\right),$$

and thus the triple product has the form

$$\begin{aligned}T_l(x)T_m(x)T_n(x) &= \frac{1}{4}\left(T_{l+m+n}(x)+T_{|l-m-n|}(x)+T_{l+|m-n|}(x)\right.\\ &\quad\left.+T_{|l-|m-n||}(x)\right).\end{aligned}$$

Using the above simple formula, we can expand the nonlinear term W^3 in (23) as follows:

$$\begin{aligned}(W(\tau,x))^3 &= \sum_{l,m,n=0}^{\infty} a_l(\tau)a_m(\tau)a_n(\tau)T_l(x)T_m(x)T_n(x)\\ &= \sum_{n=0}^{\infty} w_n(\tau)T_n(x), \end{aligned} \tag{52}$$

where

$$\begin{aligned}w_0(\tau) &:= \frac{1}{4}\left(a_0(\tau)\right)^3 + \frac{1}{4}\sum_{m=0}^{\infty} a_0(\tau)\left(a_m(\tau)\right)^2\\ &+ \frac{1}{4}\sum_{m,n=0}^{\infty}\left(a_{m+n}(\tau)+a_{|m-n|}(\tau)\right)a_m(\tau)a_n(\tau)\end{aligned} \tag{53}$$

and, for $k>0$,

$$\begin{aligned}w_k(\tau) := \frac{1}{4}\sum_{m,n=0}^{\infty}&\left(a_{k-m-n}(\tau)+a_{k-|m-n|}(\tau)+a_{k+m+n}(\tau)\right.\\ &\left.+\, a_{-k+m+n}(\tau)+a_{k+|m-n|}(\tau)+a_{-k+|m-n|}(\tau)\right)\, a_m(\tau)a_n(\tau).\end{aligned} \tag{54}$$

Here it is assumed implicitly that all coefficients with negative indices vanish identically.

In order to deal with the terms involving $x\partial_x W$ and $x\partial_{\tau x}W$ in (23) we recall that

$$xT_n'(x) = \begin{cases} n\left(2\sum_{j=0}^{n/2} T_{2j}(x) - T_0(x) - T_n(x)\right), & n=0,2,4,\ldots,\\ n\left(2\sum_{j=0}^{(n-1)/2} T_{2j+1}(x) - T_n(x)\right), & n=1,3,5,\ldots.\end{cases}$$

Thus, defining

$$z_0(\tau) := \sum_{j=0}^{\infty} 2ja_{2j}(\tau)$$

and

$$z_k(\tau) := ka_k(\tau) + 2\sum_{j=1}^{\infty}(k+2j)a_{k+2j}(\tau), \quad k>0,$$

one can write

$$x\sum_{n=0}^{\infty} a_n(\tau)T_n'(x) = \sum_{n=0}^{\infty} z_n(\tau)T_n(x). \tag{55}$$

Inserting expansion (51) into (23) and using (52) and (55), we obtain an infinite system of ordinary differential equations of the form

$$\ddot{a}_n + \dot{a}_n + (n^2-\ell(\ell+1))a_n + z_n + 2\dot{z}_n + \ell(\ell+1)w_n = 0 \tag{56}$$

for $n=0,1,\ldots$. In numerical computations we truncate this infinite system at some prescribed $n=N$ and retain the first $N+1$ coefficients $a_0,a_1,\ldots,a_N$. The truncated finite-dimensional dynamical system can be solved using standard numerical methods. This procedure is usually referred to as the Galerkin method. The initial data consist of a set of $2N+2$ values $\{a_n(0),\dot{a}_n(0)\}_{n=0,\ldots,N}$. In the computations presented in section 5 we set N of the order of 30 to 50.

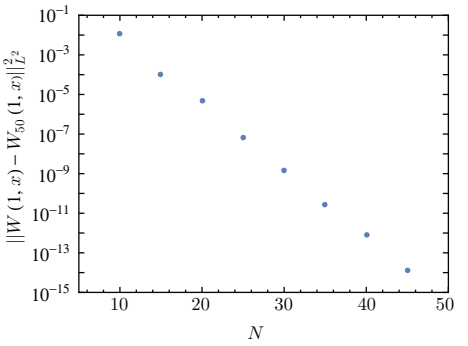

FIGURE 11. A sample convergence test of our numerical scheme. The abscissa shows the index N of the highest Chebyshev polynomial used in the computation. The ordinate shows the square of the $L^2([-1,1])$ norm of the difference between two solutions at time $\tau = 1$: the numerical solution computed with the given number of Chebyshev polynomials and the same solution computed with $N = 50$ (this solution is denoted as W_{50}). The initial data in this example are given by (46).

The convergence of our spectral numerical scheme is, as expected, exponential, at least in the cases that we have tested so far. An example of the convergence properties (with respect to the increasing number on Chebyshev polynomials used in the computation) is shown in Figure 11.

All numerical examples shown in this paper were computed with *Wolfram Mathematica*. A sample *Mathematica* notebook containing the implementation of the above method is available from the "*Mathematica* notebook demo" link at `http://dx.doi.org/10.1090/tran/6807`.

ACKNOWLEDGMENTS

The first author thanks Helmut Friedrich for helpful discussions. The second author acknowledges the hospitality of the A. Einstein Institute in Golm where this work was initiated. This research was supported in part by the NCN grant NN202 030740 and the Polish Ministry of Science and Higher Education grant 7150/E-338/M/2014.

REFERENCES

[1] Douglas M. Eardley and Vincent Moncrief, *The global existence of Yang-Mills-Higgs fields in 4-dimensional Minkowski space. I. Local existence and smoothness properties*, Comm. Math. Phys. **83** (1982), no. 2, 171–191. MR649158 (83e:35106a)

[2] Demetrios Christodoulou, *Global solutions of nonlinear hyperbolic equations for small initial data*, Comm. Pure Appl. Math. **39** (1986), no. 2, 267–282, DOI 10.1002/cpa.3160390205. MR820070 (87c:35111)

[3] Piotr Bizoń, Tadeusz Chmaj, and Andrzej Rostworowski, *Late-time tails of a Yang-Mills field on Minkowski and Schwarzschild backgrounds*, Classical Quantum Gravity **24** (2007), no. 13, F55–F63, DOI 10.1088/0264-9381/24/13/F01. MR2334886 (2008k:83074)

[4] Piotr T. Chruściel and Jalal Shatah, *Global existence of solutions of the Yang-Mills equations on globally hyperbolic four-dimensional Lorentzian manifolds*, Asian J. Math. **1** (1997), no. 3, 530–548. MR1604914 (2000b:58052)

[5] Piotr Bizoń, Andrzej Rostworowski, and Anıl Zenginoğlu, *Saddle-point dynamics of a Yang-Mills field on the exterior Schwarzschild spacetime*, Classical Quantum Gravity **27** (2010), no. 17, 175003, 11, DOI 10.1088/0264-9381/27/17/175003. MR2671555 (2011k:81209)
[6] J. A. Wheeler, *Geometrodynamics*, Academic Press, New York, 1962.
[7] Piotr Bizoń, *Formation of singularities in Yang-Mills equations*, Acta Phys. Polon. B **33** (2002), no. 7, 1893–1922. MR1923684 (2003g:58021)
[8] Kevin Corlette and Robert M. Wald, *Morse theory and infinite families of harmonic maps between spheres*, Comm. Math. Phys. **215** (2001), no. 3, 591–608, DOI 10.1007/PL00005545. MR1810946 (2002f:58015)
[9] Jan Dereziński and Michał Wrochna, *Exactly solvable Schrödinger operators*, Ann. Henri Poincaré **12** (2011), no. 2, 397–418, DOI 10.1007/s00023-011-0077-4. MR2774864 (2012c:81081)
[10] Hidekazu Nariai, *On a new cosmological solution of Einstein's field equations of gravitation [MR0055837 (14,1133f)]*, Gen. Relativity Gravitation **31** (1999), no. 6, 963–971, DOI 10.1023/A:1026602724948. MR1693455
[11] Helmut Friedrich, *Cauchy problems for the conformal vacuum field equations in general relativity*, Comm. Math. Phys. **91** (1983), no. 4, 445–472. MR727195 (85g:83005)
[12] Anıl Zenginoğlu, *Hyperboloidal foliations and scri-fixing*, Classical Quantum Gravity **25** (2008), no. 14, 145002, 19, DOI 10.1088/0264-9381/25/14/145002. MR2430521 (2009j:83022)
[13] Anıl Zenginoğlu, *A hyperboloidal study of tail decay rates for scalar and Yang-Mills fields*, Classical Quantum Gravity **25** (2008), no. 17, 175013, 13, DOI 10.1088/0264-9381/25/17/175013. MR2430682 (2010a:83055)
[14] Oliver Rinne and Vincent Moncrief, *Hyperboloidal Einstein-matter evolution and tails for scalar and Yang-Mills fields*, Classical Quantum Gravity **30** (2013), no. 9, 095009, 27, DOI 10.1088/0264-9381/30/9/095009. MR3046474
[15] B. G. Schmidt, *On relativistic stellar oscillations,* Gravity Research Foundation essay (1993).
[16] Claude M. Warnick, *On quasinormal modes of asymptotically anti-de Sitter black holes*, Comm. Math. Phys. **333** (2015), no. 2, 959–1035, DOI 10.1007/s00220-014-2171-1. MR3296168
[17] Piotr Bizoń, Tadeusz Chmaj, and Andrzej Rostworowski, *Asymptotic stability of the skyrmion*, Phys. Rev. D **75** (2007), no. 12, 121702, 5, DOI 10.1103/PhysRevD.75.121702. MR2326835 (2008c:81110)
[18] F. E. Neumann, *Beiträge zur Theorie der Kugelfunctionen*, II, Leipzig, 1878.
[19] J. C. Adams, *On the expression of the product of any two Legendre's coefficients by means of a series of Legendre's coefficients*, Proc. Roy. Soc. London **27** (1878), 63-71.
[20] P. Bizoń and M. Kahl, *Yang-Mills field on the extremal Reissner-Nordström black hole*, arXiv:1603.0475.

Institute of Physics, Jagiellonian University, Kraków, Poland – and – Max Planck Institute for Gravitational Physics (A. Einstein Institute), Golm, Germany
E-mail address: piotr.bizon@aei.mpg.de

Institute of Physics, Jagiellonian University, Kraków, Poland
E-mail address: patryk.mach@uj.edu.pl